Cell Host & Microbe
Article

T Cells Kill Bacteria Captured by Transinfection from Dendritic Cells and Confer Protection in Mice

Aránzazu Cruz-Adalia,[1,2] Guillermo Ramirez-Santiago,[1,2] Carmen Calabia-Linares,[2] Mónica Torres-Torresano,[1,2] Lidia Feo,[2] Marta Galán-Díez,[3,4] Elena Fernández-Ruiz,[3] Eva Pereiro,[5] Peter Guttmann,[6] Michele Chiappi,[7] Gerd Schneider,[6] José López Carrascosa,[7,8] Francisco Javier Chichón,[7] Gloria Martínez del Hoyo,[9] Francisco Sánchez-Madrid,[3] and Esteban Veiga[1,2,*]

[1]Centro Nacional de Biotecnología, Consejo Superior de Investigaciones Científicas (CNB-CSIC), Department of Molecular and Cellular Biology, Darwin, 3, 28049 Madrid, Spain
[2]Instituto de Investigación Sanitaria Princesa, Hospital de Santa Cristina, 28009 Madrid, Spain
[3]Instituto de Investigación Sanitaria Princesa, Hospital de la Princesa, 28006 Madrid, Spain
[4]Microbiology and Immunology Department, Columbia University Medical Center, New York, NY 10032, USA
[5]ALBA Synchrotron Light Source, MISTRAL Beamline–Experiments Division, Cerdanyola del Vallès, 08290 Barcelona, Spain
[6]Helmholtz-Zentrum Berlin für Materialien und Energie GmbH, Institute Soft Matters and Functional Materials, Electron Storage Ring BESSY II, Albert-Einstein-Strasse 15, 12489 Berlin, Germany
[7]Department Macromolecular, Centro Nacional de Biotecnología (CNB-CSIC), Darwin, 3, 28049 Madrid, Spain
[8]Instituto Madrileño de Estudios Avanzados en Nanociencia (IMDEA Nanociencia), 28049 Cantoblanco, Madrid, Spain
[9]Centro Nacional de Investigaciones Cardiovasculares (CNIC), Melchor Fernández Almagro, 3, 28029 Madrid, Spain
*Correspondence: eveiga@cnb.csic.es
http://dx.doi.org/10.1016/j.chom.2014.04.006

SUMMARY

Dendritic cells (DCs) phagocytose, process, and present bacterial antigens to T lymphocytes to trigger adaptive immunity. In vivo, bacteria can also be found inside T lymphocytes. However, T cells are refractory to direct bacterial infection, leaving the mechanisms by which bacteria invade T cells unclear. We show that T cells take up bacteria from infected DCs by the process of transinfection, which requires direct contact between the two cells and is enhanced by antigen recognition. Prior to transfer, bacteria localize to the immunological synapse, an intimate DC/T cell contact structure that activates T cells. Strikingly, T cells efficiently eliminate the transinfecting bacteria within the first hours after infection. Transinfected T cells produced high levels of proinflammatory cytokines and were able to protect mice from bacterial challenge following adoptive transfer. Thus, T lymphocytes can capture and kill bacteria in a manner reminiscent of innate immunity.

INTRODUCTION

During infections, APCs, e.g., DCs, phagocytose and process bacteria, migrate to the lymph nodes, and present bacterial antigens to naive T cells (Kaufmann and Schaible, 2005; Steinman, 1991; Waite et al., 2011). Bacterial destruction by APCs is not always complete (Cossart and Sansonetti, 2004), and it has been shown that infected DCs containing live bacteria move from infected tissues to the lymph nodes, where they are able to contact with T cells (Waite et al., 2011). Antigen presentation occurs through the formation of the immunological synapse (IS), an organized functional structure formed by the intimate contact between T cell and antigen-loaded APC (Dustin, 2008; Saito and Batista, 2010). IS formation is the main mechanism of T cell activation, is crucial for the adaptive immune response (Cemerski and Shaw, 2006; Saito and Batista, 2010), and drives major morphological changes in the T cell, including massive actin rearrangements at the cell-to-cell contact zone (Calabia-Linares et al., 2011). Moreover, the intimate contacts of APC and T cells during IS serve as platforms for exchange membranes, exosomes, and genetic material (Mittelbrunn and Sánchez-Madrid, 2012). In addition, the IS can be hijacked by some viruses (i.e., HIV). $CD4^+$ T cells are the main target of HIV, and it has been shown that HIV efficiently transinfects T cells from infected DCs (Geijtenbeek et al., 2000). The exact route of viral transinfection is not clear, and several mechanisms, including hijacking the exosome delivery pathway, have been proposed (Izquierdo-Useros et al., 2010). In this view, DCs capture HIV in the peripheral tissues and then migrate to the lymph nodes, where HIV-1 transfers toward CD4+ T cells and start the spread of infection (Geijtenbeek et al., 2000; Izquierdo-Useros et al., 2010). Some pathogenic bacteria (i.e., *Listeria monocytogenes* and *Shigella flexneri*) are also able to invade T cells in vivo (McElroy et al., 2009; Salgado-Pabón et al., 2013), and modify the behavior of the infected T cells (Salgado-Pabón et al., 2013). However, since primary T cells are poorly infected in vitro (see the Results), the route followed by pathogenic bacteria to infect T cells remained unknown. Bacterial interactions with T cells have been poorly studied, since the accepted dogma is that T cells, which drive the adaptive immunity, exert their role resolving infections in *trans*, by secreting cytokines after being specifically stimulated with the proper antigens recognized by their TCRs (Müller et al., 2012; Oykhman and Mody, 2010). Using primary cells from mice and human origin (in order to avoid cell line-derived artifacts, we decided to work with primary cells), we show unexpected roles for T cells that expand the commonly accepted functions of lymphocytes; T cells are able to take up bacteria from infected DCs

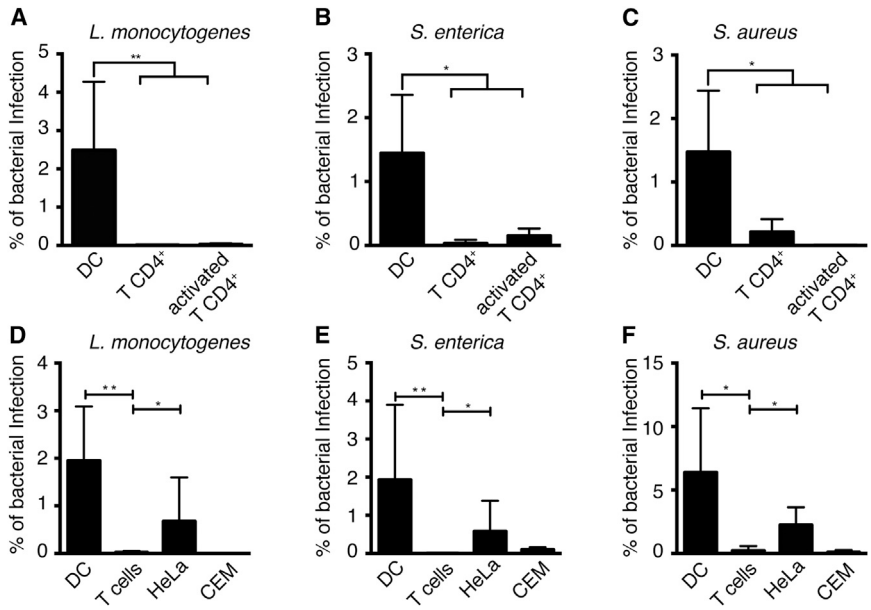

Figure 1. T Cells Are Refractory to Direct Bacterial Infection

Gentamicin survival assays showing the rate of bacterial infection of the indicated cells from mouse (A–C) and human (D–F) origin. When indicated, lymph node cells were incubated with OVAp, and after 24 hr activated $CD4^+$ T cells were isolated. The column bars represent the mean of at least three independent experiments. Error bars indicate the SD. Significant differences are represented by asterisk.

(bacterial transinfection) and then efficiently kill them, similarly to cells of the innate immune system. Transinfected T cells secrete larger amounts of proinflammatory cytokines (IL-6, interferon-γ and, TNF-α) that have been known from long to play an important role in bacterial elimination in vivo (Nakane et al., 1992) than noninfected T cells, and block bacterial infection in vivo.

RESULTS

Primary T Cells Are Refractory to Direct Bacterial Infection

Three different bacteria species (*Salmonella enterica* serovar *enteritidis*, *Listeria monocytogenes*, and *Staphylococcus aureus*) were used to infect naive or antigen-activated $CD4^+$ T cells isolated from mice lymph nodes. All three bacteria infected $CD4^+$ T cells very poorly compared to LPS-activated, mature, bone marrow-derived DCs (Figures 1A–1C). Similar results (poor bacterial infections) were observed using human primary T lymphoblasts compared to monocyte-derived DCs or HeLa cells, used as positive controls (Figures 1D–1F). These data reveal that primary T cells are refractory to direct bacterial infection. These data, together with the fact that bacteria can be found inside T cells in vivo, prompted us to hypothesize that bacteria could transinfect T cells from infected APCs during antigen presentation.

Bacteria Infecting DCs Localized at the IS Shortly after T Cell Contact

We imaged the subcellular localization of bacteria during the formation of the IS between infected DCs contacting noninfected T cells (Figure 2). Mouse bone marrow-derived dendritic cells (mDCs) loaded with OVA peptide (OVAp) were infected with *L. monocytogenes*, *S. enterica*, or *S. aureus* and coincubated with $CD4^+$ T cells from transgenic OTII mice, which bear a TCR specific for OVAp (Barnden et al., 1998). Bacteria polarized toward the DC-T cell contact area during IS formation (Figures 2A–2C). Similar observations were made using infected human monocyte-derived DCs (hDCs) loaded with superantigen E (SEE) and human T lymphoblasts recognizing SEE (TCR bearing $V\beta8^+$ chains [Niedergang et al., 1998]) (Figures 2D–2F). The formation of active IS was confirmed by the polarization of the microtubules organizing center (MTOC) and CD3 (see Figure S1 available online). Note that protein accumulation in the IS in primary cells is less evident than using cell lines (Reichardt et al., 2010). Polarization of bacteria during IS formation was confirmed by live cell imaging (Figures 2G and S2A; Movie S1 and Movie S2). Moreover, bacteria were able to transinfect T cells from contacting infected DCs (Figures 2H and S2B–S2G; Movie S3, Movie S4, Movie S5, and Movie S6). Bacterial localization in the IS was further confirmed by high-resolution cryo-Soft X-ray tomography (cryo-SXT) (Figures 2I and 2J; Movie S7). This unconventional technology allows the imaging of whole cells maintained frozen in their native state avoiding the artifacts of fixation and sectioning, and without the use of any contrasting agent (Schneider et al., 2010).

T Cells Take Up Bacteria by Transinfection from DCs

The process of bacterial transinfection from infected DCs toward contacting T cells was quantified by T cells' reisolation after conjugate formation, followed by classical gentamicin survival assays (Pizarro-Cerda and Cossart, 2010; Vaudaux and Waldvogel, 1979). This sensitive method allowed us to analyze a large number of conjugates. The requirement of cell-to-cell contact was tested by using polycarbonate filter-containing chambers impeding cellular contact between infected DCs and T cells and the role of antigen presentation by loading DCs with OVAp or SEE for mouse or human cells, respectively (Figure S3A). Regarding the mouse-cell model, the maximal bacterial uptake by $CD4^+$ T cells occurs when cell-to-cell contact is allowed and infected DCs presented OVAp (Figures 3A–3C), which is consistent with IS-mediated bacterial transinfection and was similar for the three bacteria tested. When cell-to-cell contacts were impeded, the infection was very low and similar to direct incubation of the bacteria with the $CD4^+$ T cells (negative control). Only experiments with purity >97% of the reisolated T cells were taken into account (Figure 3D), and the colony-forming units (CFUs) from the contaminants were subtracted. The relevance of antigen presentation during transinfection

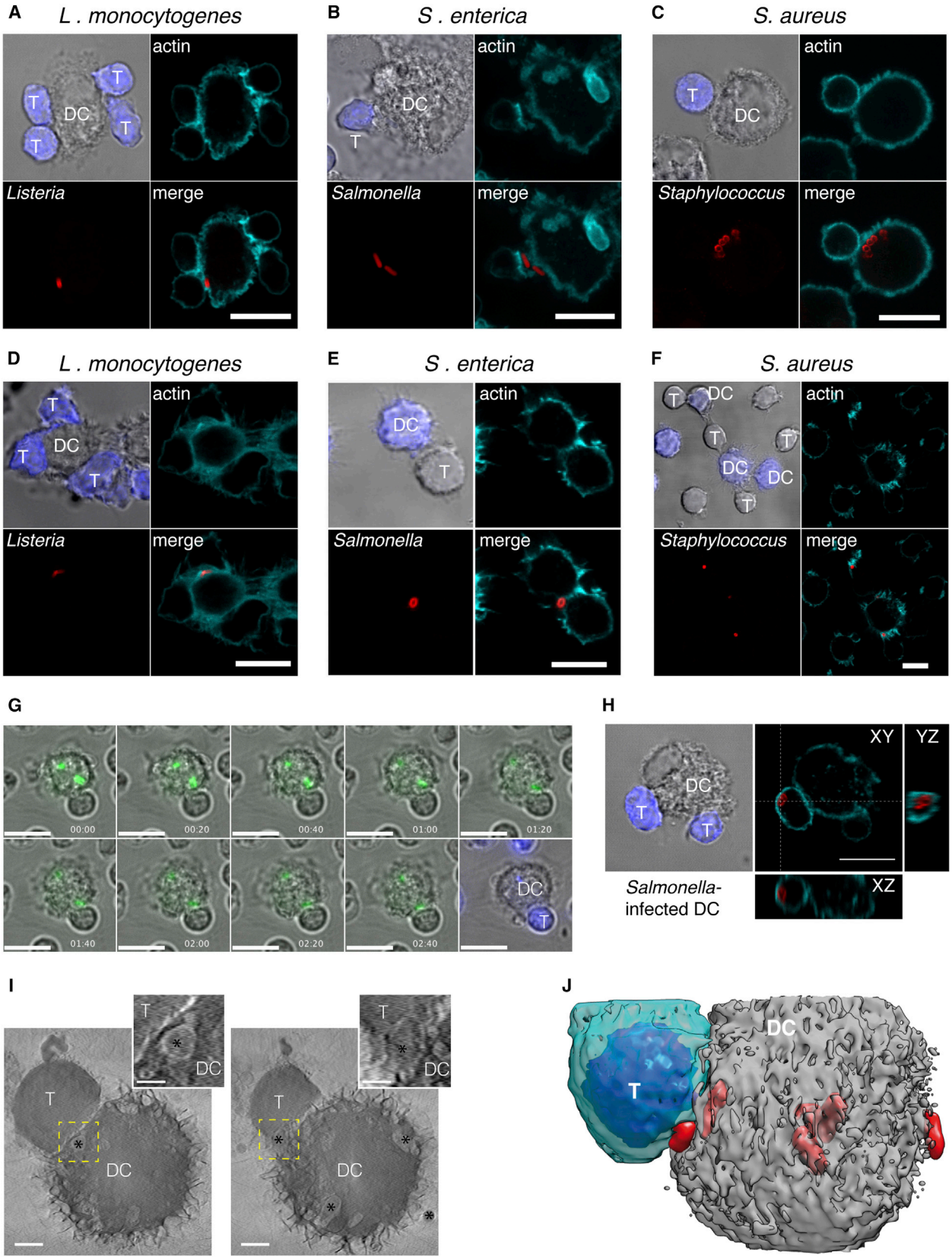

(legend on next page)

was additionally confirmed by flow cytometry. After conjugate formation, intracellular bacteria in $CD4^+$ T cells were detected by differential immunolabeling (Figure S3B). The maximal bacterial uptake by $CD4^+$ T cells occurred when DCs presented OVAp (Figure 3E). To further confirm this, infected DCs were allowed to form conjugates simultaneously with both $CD4^+$ T cells isolated from wild-type mice (with no specificity for OVAp) and OT-II mice (OVAp specific). Infection was reduced in T cells isolated from wild-type mice (Figure 3F), demonstrating that antigen specificity enhanced bacterial transfer. Note that bacterial association with DCs was unaffected by the presence of antigen (Figure S4A), and preactivation of T cells has no effect in bacterial transinfection (Figure S4B). Moreover, the presence of anti-LFA-1, previously described to block partially cell-cell conjugate and IS formation (Sanchez-Madrid et al., 1983), reduced bacterial spreading (Figure 3G). Transinfection of nonpathogenic *Escherichia coli* (DH5α) was similar to that observed with pathogen species (Figure S4C); thus, virulence factors do not seem to be strictly necessary for this process.

In order to test whether bacterial transinfection also occurs in $CD8^+$ T cells, we used $CD8^+$ T cells isolated from OT-I transgenic mice, which produce MHC class I-restricted, specific for the ovalbumin peptide (257–264) (Hogquist et al., 1994). As observed in $CD4^+$ T cells, transinfection requires cell-to-cell contact and was maximal in the presence of antigen (Figure 3H).

Similar results were observed in the human-model using SEE as antigen (Figures 4A–4C); maximal bacterial transfer (for all bacteria tested) was observed when cell-to-cell contact was allowed and in the presence of antigen. T cell infection rates were higher in the human-cell model, probably as a consequence of strong T cell activation produced by superantigens (Niedergang et al., 1998). Figure 4D shows the purity of the reisolated T cells from a representative experiment; note that only experiments with purity >97% were taken into account, and the CFUs from the contaminants were subtracted. The relevance of antigen presentation was confirmed by flow cytometry experiments (Figure 4E). Moreover, bacterial transinfection of T cells was also reduced by anti-human LFA-1 antibody (Campanero et al., 1993) (Figure 4F). To further confirm that antigen-dependent contact is necessary for bacterial transinfection to occur, and that transinfection is not only due to sustained cell-to-cell contact, we forced infected DC to contact T cells using an aggregation-inducer anti-CD43 antibody (Serrador et al., 1998). However, engagement of CD43, that induced massive cellular aggregates (data not shown), did not increase the number of transinfected bacteria in T cells (Figure S4D). A nonpathogenic mutant strain of *S. aureus* lacking the sortase gene (Δ*srt*) (Vergara-Irigaray et al., 2009) was also efficiently transferred to human T cells when IS formation was allowed (Figure S4E), demonstrating again that virulence factors do not seem to be strictly necessary for bacterial transfer from DCs to T cells. Additionally, we showed that this process was specific for bacteria and not for any phagocytosed particle by incubating DC with fluorescent polystyrene beads. T cells were unable to take up beads from DCs (Figure 5A), despite the fact that more DCs appeared associated with beads than with bacteria (Figure S4F) and that T cells were able to capture beads directly from the medium (Figure 5A). In addition, DCs were incubated with beads, or with beads and *L. monocytogenes* at the same time (with no differences in beads uptake by DC; data not shown). The presence of bacteria did not increase the capture of beads by T cells (Figure 5B). All these data show that during IS formation T cells are able to specifically take up bacteria from DCs.

Bacterial Transinfection Requires Active T Cell Cytoskeleton

The IS formation triggers dramatic changes in the cytoskeleton of T cells (Calabia-Linares et al., 2011; Gomez et al., 2005). Interestingly, T cells actively extend pseudopodia toward the infected DCs (Movie S2, Movie S3, Movie S4, and Movie S5), in agreement with recent observations (Ueda et al., 2011). To study whether the T cell cytoskeleton participates in bacterial uptake through the IS, we incubated T cells with either cytochalasin D or colchicine to disrupt the actin filaments or the microtubules, respectively. Either drug inhibited T cell bacterial uptake from infected DCs in the human and murine models (Figures 5C, 5D, and S5), indicating that T cell cytoskeleton plays a major role in this process.

T Cells Uptake Both Intracellular and Surface-Exposed Bacteria from Infected DCs

To determine whether T cells capture bacteria from the inside or associated to the surface of the DCs, we used gentamicin to kill extracellular bacteria. In the presence of gentamicin (condition 1), only intracellular translocation of bacteria was allowed. When gentamicin was washed out before conjugation with T cells, DCs intracellular bacteria were able to translocate to T cells either directly from inside of DCs to the interior of T cells or through an extracellular step before entering T cells (condition 2). In the absence of gentamicin (condition 3), both extracellular and intracellular, bacterial transfers were allowed (Figure S6A). Maximum uptake of *L. monocytogenes* by T cells was observed in condition 3 (2-fold compared to

Figure 2. Bacteria Localize at the IS Shortly after Conjugate Formation

(A–F) confocal images of antigen-loaded DCs infected with the indicated bacteria (red) coincubated during 30 min with noninfected primary T cells. Actin is shown in cyan. (A–C) mDCs (not stained) and mouse $CD4^+$ T cells (blue) are shown. Human T lymphoblasts are shown in blue (D) or nonstained (E and F). hDCs are shown in blue (E and F) or not stained (D).

(G) Live-cell time series showing the contact between *S. enterica*-GFP-infected mDC and T cell from Movie S1.

(H) Orthogonal view of sample as in (B), with *S. enterica* inside transinfected T cell. Bars represent 10 μm in (A–H).

(I) Virtual slices of a cryo soft X-ray tomogram acquired at BESSY-II from a T cell (T) interacting with an *S. enterica*-infected DC. The asterisks mark the position of *Salmonella*. The indicated bacteria are inside DC close to the IS (left) and outside DC and being engulfed by the T cell (right). Inset shows a detailed position of bacteria. Scale bars represent 2 micron and 1 micron in the insets.

(J) Volumetric representation of the cryo soft X-ray tomogram shown in (I). Bacteria are represented in red, T cell in cyan, and DC in gray. The nucleus of the T cell is shown in blue.

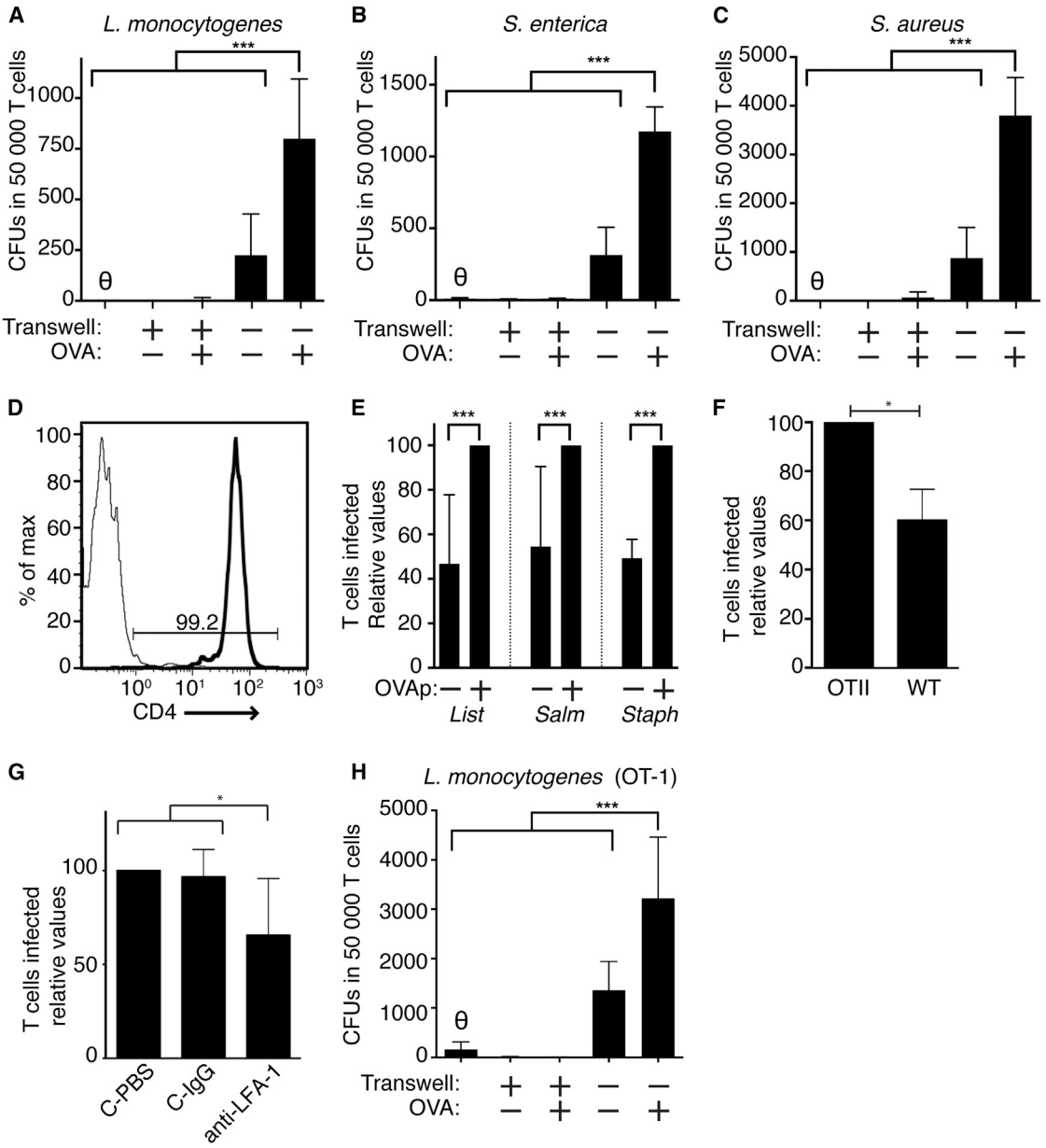

Figure 3. Bacterial Transinfection Is Enhanced by Antigen Presentation

(A–C) mDC were loaded (or not) with OVAp (OVA) and infected with the indicated bacteria, followed by coincubation with $CD4^+$ T cells in conditions that allow DC-T cell interactions for 30 min, or in the presence of a polycarbonate barrier (transwell) impeding such interactions. After conjugate formation, $CD4^+$ T cells were reisolated, and classical gentamicin survival assays were performed. Shown are the CFUs corresponding to 50,000 $CD4^+$ T cells. θ indicates direct infection of bacteria in T cells.

(D) Representative experiment of flow cytometry showing the purity of reisolated T cells before performing gentamicin survival assay. Thick line shows the percentage of $CD4^+$ cells, and thin line shows the antibody negative control.

(E) The rate of $CD4^+$ T cells harboring intracellular bacteria (CD11c−, CMAC+, extracellular bacteria−, total bacteria+) was determined by flow cytometry.

(F) OVAp-loaded, *Salmonella*-infected DCs were coincubated with a mix (ratio 1:1) of $CD4^+$ T cells from OT-II and WT mice (stained differentially with CMAC). $CD4^+$ T cell populations were differentiated by flow cytometry. Infection of OT-II T cells was taken as 100%.

(G) *S. enterica*-infected and OVAp-loaded mDCs were treated with anti LFA-1 antibody (M17/4), control isotype IgG, or just PBS before coincubation with T cells. T cell infection rate in nontreated samples was taken as 100%.

(H) Similarly to (A)–(C) but using $CD8^+$ T cells isolated from OT-I mice and conjugated with mDCs loaded with its specific OVA peptide.

Column bars represent the mean of at least three independent experiments. Error bars indicate the SD. Significant differences are represented by asterisk.

condition 2). In condition 1, T cells acquired approximately 50% of bacteria they took up in condition 2 (Figure 5E). These data show that T cells captured both extracellular and intracellular *L. monocytogenes* from DCs, and that intracellular bacteria were able to undergo an extracellular step before entering T cells.

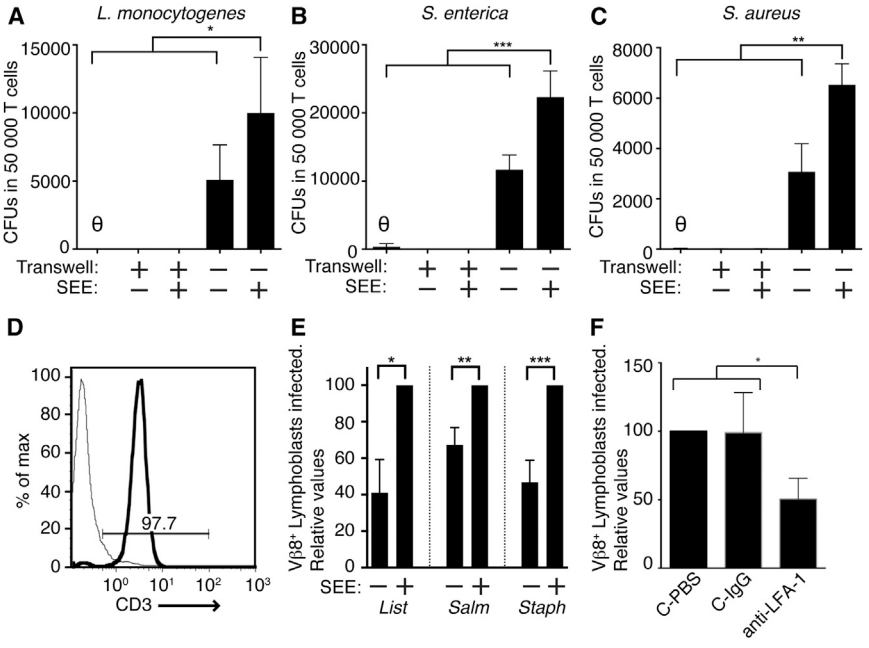

Figure 4. Bacterial Transinfection in Human Cells Model

(A–C) hDC were loaded (or not) with SEE and infected with the indicated bacteria followed by coincubation with Vβ8$^+$-enriched T lymphoblasts in conditions that allow DC-T cell interactions, or in the presence of a polycarbonate barrier (transwell) impeding such interactions. After conjugate formation, T cells were reisolated, and classical gentamicin survival assays were performed. Shown are the CFUs corresponding to 50,000 T cells. θ indicates direct infection of bacteria in T cells.

(D) Representative experiment of flow cytometry showing the purity of reisolated T cells before performing gentamicin survival assay. Thick line shows the percentage of CD3$^+$ cells; thin line shows the antibody negative control.

(E) The rate Vβ8$^+$ T lymphoblasts harboring intracellular bacteria (DC-SIGN−, Vβ8$^+$, extracellular bacteria−, total bacteria+) was determined by flow cytometry.

(F) SEE-loaded, *Salmonella*-infected hDCs were incubated with anti LFA-1 antibody (Lia3.2), control isotype IgG, or just PBS before coincubation with T lymphoblasts. The rate of T lymphoblasts infected in nontreated samples was taken as 100%.

Column bars represent the mean of at least three independent experiments. Error bars indicate the SD. Significant differences are represented by asterisk.

T Cells Eliminate Uptaken Bacteria

L. monocytogenes-OVA (expressing the OVA protein in the bacterial surface) transinfected OT-II T cells ex vivo (Figure S6B). In order to test whether bacteria could transinfect T cells in vivo, OT-II mice were injected intravenously with *L. monocytogenes* and *L. monocytogenes*-OVA, and 24 hr after infection CD4$^+$ T cells were harvested from the spleen and the presence of bacterial CFUs was assessed by standard gentamicin survival assay. *L. monocytogenes*-OVA transinfected CD4$^+$ T cells more efficiently than *L. monocytogenes* nonexpressing OVAp (Figure 6A) (note that no differences in bacterial infection were found between *L. monocytogenes*-OVA and WT *L. monocytogenes* when WT C57BL/6 mice were infected; data not shown). Surprisingly, the amount of recovered bacteria was extremely low compared to what was observed ex vivo. This striking result prompted us to assess the fate of bacteria inside T cells. To address this, OVAp-loaded mDCs were infected with either *L. monocytogenes* or *S. enterica* and conjugated with CD4$^+$ T cells from OTII mice. After conjugate formation, T cells were reisolated and CFUs were analyzed by gentamicin survival assays at different times. Unexpectedly, T cells rapidly killed the internalized bacteria (Figure 6B). Within the first hours after conjugate formation, more than 95% of the internalized *L. monocytogenes* and 90% of *S. enterica* were killed. As control for bacterial fitness, we measured CFUs after direct infection of HeLa cells (Figure 6C). No apparent damage of T cells was appreciated during the time course of the experiment. Similar results were observed in the human model: after bacteria transinfection, human T cells rapidly killed intracellular bacteria. Within the first hours after conjugate formation, more than 95% of the internalized *L. monocytogenes* were killed (Figure 6D).

In order to determine the cellular mechanisms involved in bacterial destruction, T cells were treated with different inhibitors before conjugate formation. As shown (Figure 6E), Pepstatin A, an inhibitor of aspartyl proteases and NH_4Cl which inhibits phagosome-lysosome fusion, partially inhibited intracellular bacterial degradation, suggesting that lysosome degradation plays an important role in intracellular bacterial clearance in T cells. On the contrary, MnTBAP and NAC inhibiting production of oxygen reactive species, 1400W, a potent and selective inhibitor of iNOS and L-NAME, an arginine analog inhibiting NO production, did not impede bacterial degradation inside T cells.

These results clearly show a role for CD4$^+$ T lymphocytes during bacterial infections being able to internalize and clear the bacteria in a lysosome-dependent way.

Role of Transinfection in Bacterial Clearance

To further test the physiological relevance of this phenomenon, we analyzed first the cytokines secreted by CD4$^+$ T cells from OT-II mice transinfected with *L. monocytogenes*. In order to optimize the number of T cells transinfected, we allowed conjugate formation for 24 hr. T cells were reisolated and stimulated with anti-CD3 and anti-CD28 antibodies, and then the production of cytokines was quantified by cytometric bead array (CBA; Figure 7A). Transinfected CD4$^+$ T cells secrete higher amounts of IL-6, interferon-γ, and TNF-α (typical proinflammatory cytokines) than noninfected CD4$^+$ T cells.

To assess whether transinfection, and therefore bacteria killing and inflammatory cytokine secretion by CD4$^+$ T cells, plays a role in bacterial clearance during in vivo infections, we performed adoptive transfer experiments. CD4$^+$ T cells from OT-II (responding to OVA) or WT mice (not responding to OVA)

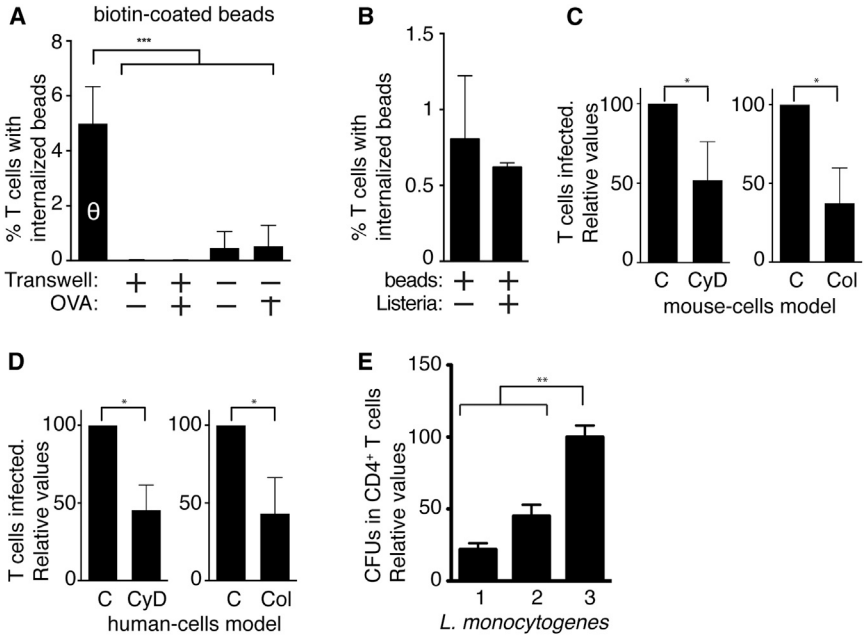

Figure 5. Transinfection Requires Active Cytoskeleton of T Cells

(A) mDC were loaded (or not) with OVAp and fluorescent, biotin-coated microspheres. Then mDCs were coincubated with CMAC-stained $CD4^+$ T cells in conditions that allow DC-T cell interactions, or in the presence of a polycarbonate barrier (transwell). $CD4^+$ T cells harboring intracellular beads (CD11c−, CMAC+, extracellular beads−, total beads+) were detected by flow cytometry. θ indicates direct addition of beads to T cells.

(B) OVAp-loaded DC cells were incubated with fluorescent, biotin-coated microspheres together (or not) with *L. monocytogenes*. After 1 hr coincubation with $CD4^+$ T, the internalization of microspheres by T cells was analyzed by flow cytometry.

(C and D) (C) Mouse T cells or human $V\beta8^+$-enriched T lymphoblasts (D) were treated with cytochalasin D (CyD) or colchicine (Col), 30 min before coincubation with *S. enterica*-infected and antigen-loaded DCs. Infection observed (by flow cytometry) in controls was taken as 100%.

(E) Listeria-infected and OVAp-loaded mDCs were coincubated with $CD4^+$ T cells from OTII mice. In condition 1, gentamicin was added before and maintained during conjugate formation. In condition 2, gentamicin was removed before coincubation. In condition 3, no gentamicin was added. After coincubation, $CD4^+$ T cells were reisolated, and gentamicin survival assay was performed. After normalization, CFUs observed in condition 3 were taken as 100. Column bars represent the mean of at least three independent experiments. Error bars indicate the SD. Significant differences are represented by asterisk.

were transferred into WT mice and tested for bacterial load in spleen and liver after bacterial (*Listeria*-OVA) challenge. In the first set of experiments, bacterial load was tested 24 hr after challenge. Here, we included one additional condition, OT-II $CD4^+$ T cells transinfected with bacteria before being transferred into WT mice, to assure a large number of transinfected T cells. As shown (Figures 7B and 7C), transfer of both infected and noninfected OT-II T $CD4^+$ cells protects slightly from bacteria, in both spleen and liver. Transfer of WT $CD4^+$ T cells also protects from bacteria, but in a lesser extent than infected OT-II $CD4^+$ T cells. The protection of OT-II $CD4^+$ T cells was more evident at 48 hr after bacterial challenge (Figures 7D and 7E). In this case we assume that OT-II $CD4^+$ cells were able to capture and destroy a large number of bacteria, and therefore we transferred only noninfected $CD4^+$ T cells. We recovered ten times less bacteria from mice transferred with OT-II $CD4^+$ cells than from mice treated with PBS or transferred with WT T cells.

DISCUSSION

Our data show that T cells are able to trap (from infected DC) and clear bacteria, behavior thought to be exclusive for cells of the innate immunity. We have found that T cells capture bacteria by transinfection from previously infected DCs during the course of antigen presentation, this pathway being much more efficient than direct bacterial infection on T cells. This applies also to nonpathogenic strains, indicating that virulence factors are not necessary and that T cells actively guide this pathway. This is further supported by the fact that T cell cytoskeleton is necessary for bacterial uptake. Some viruses, such as HIV, use a similar transinfection pathway, from infected DC toward T cell (Izquierdo-Useros et al., 2010); it therefore appears that the IS is a major platform to T cell infection. Our data show that T cells specifically take up bacteria, but not any particle present in DCs (i.e., latex beads). It seems that T cells recognize bacterial components when bacteria are associated to DCs, as shown by the fact that T cells did not take up beads even in the presence of bacteria. The possible role of T cells PRRs (pattern recognition receptors) in transinfection and further cytokine secretion remains to be elucidated.

Unexpectedly, T cells kill intracellular bacteria (similarly to professional phagocytes) and did it more efficiently than DCs (Figure S6C). This striking result shows that cells of the adaptive immunity can support functions similar to those of the innate immunity. Moreover, transinfected $CD4^+$ T cells secrete more inflammatory cytokines than noninfected (but activated) ones. These roles of $CD4^+$ T cells in bacterial uptake and killing, together with proinflammatory cytokine secretion and therefore recruitment and activation of cells of the innate immune system, result in potent weapons in the antibacterial fight, confirmed by in vivo experiments. *Listeria* infection in the spleen normally would develop toward chronic infection unless adaptive T cell response takes place. Adaptive T cell response is usually observed later (more than 3 days after challenge) (Bregenholt et al., 2001; Waite et al., 2011); therefore the rapid antibacterial activity we observed indicates that bacterial transinfection may play an important role in this rapid T cell-driven antibacterial clearance. Our data are in accordance with previous observations, showing that proinflammatory cytokine response is important in *Listeria* elimination (Dai et al., 1997; Ehlers et al., 1992; Nakane et al., 1992).

In the present manuscript, we focused on the role of $CD4^+$ T cells during bacterial transinfection; however, the DC could also play a pivotal role. The DC-T cell interaction is absolutely

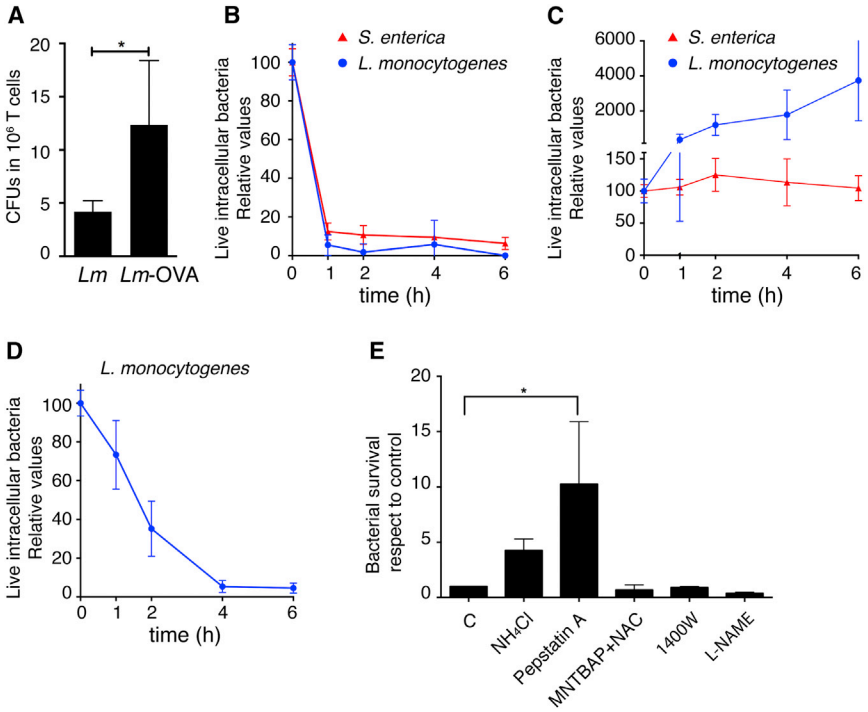

Figure 6. T CD4⁺ Cells Efficiently Kill Transinfected Bacteria

(A) OTII mice were injected with *L. monocytogenes* WT *(Lm)* or *L. monocytogenes*-OVA (Lm-OVA). Twenty-four hours after bacterial challenge, CD4⁺ T cells were isolated from spleen, and intracellular live bacteria (CFUs) were detected by gentamicin survival assays.

(B and C) (B) Bacteria-infected and OVAp-loaded mDCs were coincubated with CD4⁺ T cells from OTII mice. After conjugate formation, CD4⁺ T cells were reisolated, and intracellular bacteria were detected by gentamicin survival assays at different times. Data were normalized with respect to that observed in time 0. As control of the bacterial fitness, in parallel, HeLa cells were directly infected (C).

(D) *L. monocytogenes* survival inside human T lymphoblasts. Experiments were performed as in (B), but using human T lymphoblasts and infected SEE-loaded hDCs.

(E) Mouse CD4⁺ T cells were treated with the indicated inhibitors, before coincubation with *L. monocytogenes*-infected and antigen-loaded DCs.

After conjugate formation, CD4⁺ T cells were reisolated and maintained in medium containing the inhibitors. Bacterial survival was tested by gentamicin survival assays, and survival rate was obtained comparing the CFUs counted at time 0 (bacterial entry) with CFUs counted in samples tested 2 hr after conjugate formation. Survival rate of control cells was arbitrarily considered as 1. Column bars represent the mean of at least three independent experiments. Error bars indicate the SD. Significant differences are represented by asterisk.

necessary for transinfection to occur, and antigen presentation greatly increases the number of bacteria inside T cells. In addition, bacterial movement inside DC polarizing toward the IS could be somehow driven by the DC itself. For example, in Movie S5, bacteria seem to move toward contacting T cell using the same pathway inside the infected DC. However, bacterial transinfection by MyD88 KO DCs shows no difference compared to that observed in WT DCs (Figure S6D), indicating that DCs PRRs do not seem to play any role in bacterial transinfection.

Our data clearly show that CD4⁺ T cells eliminate the uptaken bacteria, opposite to what was previously described, showing that lymphocytes could be a reservoir for bacteria (McElroy et al., 2009). These apparent contradictory data can be explained by the fact that the authors do not distinguish between T and B cells, while in our study we focused mainly in the role of CD4⁺ T cells. In addition, as occurs with professional phagocytes, not all the bacteria are destroyed. Our findings also open the field for future research regarding the mechanisms used by T cells to eliminate intracellular pathogens as well as the possible mechanisms employed by bacteria to avoid their killing. It is also very intriguing that bacteria like *L. monocytogenes* possess several putative virulence factors with unknown functions and with unknown time-programming and localization expression patterns during the course of an infection (Cossart, 2011). A full comprehension of this phenomenon would be necessary to evaluate the bacterial expression pattern during hosting inside T cells, and to analyze whether bacteria develop mechanisms to survive inside T cells.

This manuscript shows cryo-SXT images in bacteria-host interaction. Due to the size of the bacteria, these high-resolution, nonstandardized technology results are especially useful in these studies. Cryo-SXT is capable of imaging cellular organization and locating subcellular structures in whole, hydrated cells, thus eliminating the artifacts from embedding, dehydration, and sectioning, and allowing the in situ imaging of whole cells (Schneider et al., 2010). In Movie S8, a 3D reconstruction from a tomogram acquired at the synchrotron ALBA, we can appreciate the subcellular structures like the *Salmonella*-containing vacuole (SCV).

In sum, this work discovered roles for T cells during the course of bacterial infections and paved the way for future research in the field of T cell-pathogen interactions.

EXPERIMENTAL PROCEDURES

Bacterial Strains

The bacterial strains used were *Listeria monocytogenes* (EGD; BUG600), *L. monocytogenes* cGFP (BUG2539) (Balestrino et al., 2010), *L. monocytogenes*-OVA (pPL2-LLO-OVA), a *Listeria* strain expressing OVA protein in bacterial surface (Pope et al., 2001), its WT isogenic strain *L. monocytogenes* 10403S. *Salmonella enterica* sv *enteritidis* 3934, S. enterica/pGFPmut3, *Staphylococcus aureus* 132, *S. aureus*/pCN47-GFP, *S. aureus* 132 Δsrt (mutant in sortase and therefore nonpathogenic) (Charpentier et al., 2004; Cormack et al., 1996; Solano et al., 2002; Vergara-Irigaray et al., 2009), *Escherichia coli* DH5α, and *E. coli* DH5α/pGFPmut3. Bacteria were grown in BHI (*Listeria* and *Staphylococcus*), or LB (*E. coli* and *S. enterica*). When necessary, 10 μg/ml of erythromycin or 100 μg/ml of ampicillin was added.

Mice

Wild-type C57BL/6 mice, C57BL/6-Tg *(TcraTcrb)425Cbn*/J OTII mice expressing a T cell receptor (TCR) specific for peptide 323–339 of OVA in

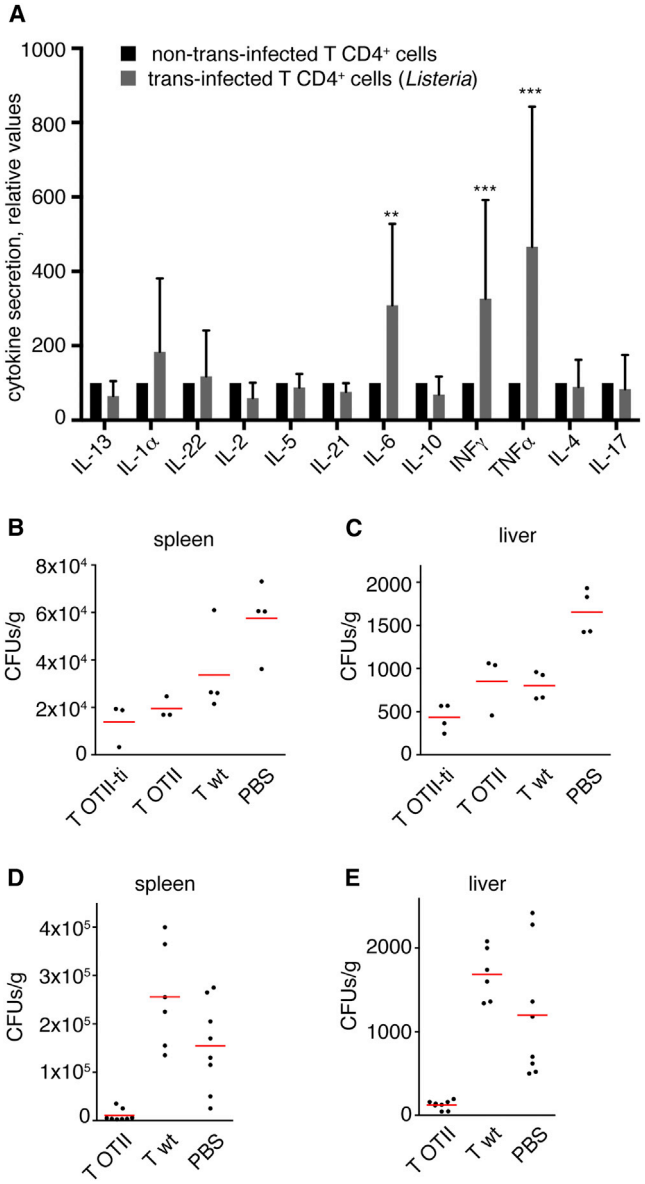

Figure 7. Transinfected T CD4$^+$ Cells Secrete More Proinflammatory Cytokines than Nontransinfected Ones

(A) CD4$^+$ T cells were activated by OVAp-loaded DCs and transinfected with *L. monocytogenes*. CD4$^+$ T cells were then reisolated and activated for 3 days with anti-CD3 and anti-CD28 antibodies. Extracellular cytokines were detected by flow cytometry using antibody-coupled beads. The data represent relative values respect to nontransinfected T cells.

(B–E) Wild-type (wt) mice were inoculated intravenously with CD4$^+$ T cells isolated from OT-II mice, from WT mice, or with PBS. In (B) and (C), OT-II CD4$^+$ T cells transinfected with *Listeria*-OVA were also inoculated. Twenty-four hours after T cells inoculation, mice were challenged with *Listeria*-OVA. Twenty-four hours (B and C) or 48 hr (D and E) after bacterial challenge, mice were sacrificed, and the bacterial load in spleen and liver was detected by CFU counting.

the context of I-A^b, and C57BL/6-Tg*(TcraTcrb)1100Mjb/J* OTI mice expressing TCR specific for peptide 257–264 of OVA in the context of H2Kb were purchased from Jackson Laboratory (stock number 004194 and 003831, respectively). Either male or female mice aged between 8 and 12 weeks were used for the experiments. Mice were kept in pathogen-free conditions at the Animal Unit of the School of Medicine, Universidad Autónoma de Madrid. Experimental procedures were approved by the Committee for Research Ethics of the Universidad Autónoma de Madrid and conducted under the supervision of the Universidad Autónoma de Madrid Head of Animal Welfare and Health in accordance with Spanish and European guidelines. Femurs from MyD88 KO mice and its isogenic C57BL/6 were provided by Bernhard Ryffel (CNRS Orleans, France).

Primary Cells and Cell Lines

Mouse Cells

DCs (mDCS) were generated according to the basic method of Inaba et al. (1992) with some modifications. Briefly, bone marrow was flushed from the tibias and femurs of 8- to 20-week-old C57BL/6 mice. Red blood cells were lysed, and the cell suspension was washed and filtered to remove debris. Bone marrow cells were seeded in P150 plates at a concentration of 5 × 10^5 ml^{-1} in RPMI 1640 supplemented with 10% fetal serum (FCS), glutamine (2 mM), 2ME (5 × 10^{-5} M), and GM-CSF (20 ng/ml). Fresh medium with GM-CSF was replaced at days 3, 6, and 9. Phenotypic characteristics of these cells were assessed by flow cytometry on day 10 (CD11c$^+$, IA/IE$^+$, and Gr1$^-$) to ensure correct differentiation. Maturation was induced with 20 ng/ml lipopolysaccharide (LPS) for 24 hr.

Primary mouse CD4$^+$ T cells were obtained from single-cell suspensions of lymph nodes (LN) from OTII mice. Cell suspensions were incubated with biotinylated antibodies against CD8, IgM, B220, CD19, MHC class II (I-Ab), CD11b, CD11c, and DX5 and subsequently with streptavidin microbeads. CD4$^+$ T cells were negatively selected in auto-MACS Pro Separator (Miltenyi Biotec) according to the manufacturer's instructions. To isolate CD8$^+$ T cells from OT-I mice, cell suspensions of lymph nodes were incubated with the same biotinylated antibodies, but instead of CD8, CD4 antibody was used.

Human Cells

Monocytes were purified from peripheral blood mononuclear cells (PBMCs) by a 30 min adherence step at 37°C in RPMI supplemented with 10% fetal calf serum. Monocytes were immediately subjected to the DC differentiation protocol, as described (Sallusto and Lanzavecchia, 1994). Briefly, monocytes were cultured in RPMI, 10% FCS containing IL-4 (500 U/ml) and GM-CSF (500 U/ml). Cells were cultured for 6 days, with cytokine readdition every 48 hr, to obtain a population of immature hDCs. Phenotypic characteristics of these cells were assessed by flow cytometry on day 6 (HLA-DR$^+$, CD3$^-$, DC-SIGN$^+$ CD14$^-$ CD1a$^+$). Maturation was induced with 1 μg/ml LPS for 24 hr.

Peripheral blood lymphocytes were isolated from PBMCs by two rounds of plastic adherence. Human enriched Vβ8$^+$ T lymphoblasts were obtained from 7 day culture with 0.1 μg/ml staphylococcal enterotoxin E-stimulated peripheral blood lymphocytes. Studies were performed according to the principles of the Declaration of Helsinki and were approved by the local Ethics Committee for Basic Research; informed consent was obtained from all human volunteers.

Cells Lines

CEM CCL-119 (human T cell lymphoblast-like cell line) were cultured in complete medium (RPMI 1640 and 10% FCS). HeLa CCL-2 were cultured in complete medium (DMEM and 10% FCS).

Antibodies and Reagents

Antibodies Recognizing Mouse Proteins

Antibodies recognizing mouse proteins included anti- CD11c, IA/IE, Gr1 (BD); biotinylated antibodies against CD3, CD4, CD8, CD28, IgM, B220, CD19, MHC class II (I-Ab), CD11b, CD11c DX5, and CD16/CD32 (BD); and anti-tubulin FITC-conjugated (Sigma). Anti-LFA-1 M17/4 and anti-CD3 were described previously (Sanchez-Madrid et al., 1983).

Antibodies Recognizing Human Proteins

Antibodies recognizing human proteins included anti-HLA-DR, anti-CD3, anti-CD1a, anti-DC-SIGN, anti-CD14, TCR chain vβ8 (BD), biotinylated DC-SIGN and CD1a (Miltenyi Biotec), LFA-1 β subunit (CD18) Lia 3/2 mAb, and CD43 (HP2/21) (Sánchez-Mateos et al., 1995; Serrador et al., 1998). Anti-DC-SIGN-alexa 647 conjugated was from AbD Serotec.

Antibodies Recognizing Bacteria

Antibodies recognizing bacteria included anti-*S. enterica*, anti-*S. aureus*, and anti-*L. monocytogenes* (ABD Serotec).

Other Reagents

OVAp (OVA 323-339; I S Q A V H A A H A E I N E A G R, and OVA 257-264; S I I N F E K L) were generated in the Centro de Biologia Molecular Severo Ochoa-CSIC), Staphylococcal Enterotoxin E (SEE, Toxin Technologies), mouse GM-CSF (Peprotech), human GM-CSF (Agrenvec), human IL-4 (R&D Systems), LPS (Sigma-Aldrich), streptavidin microbeads (Miltenyi Biotec), and Alexa Fluor 568-Phalloidin (Invitrogen). Secondary antibodies anti-mouse and anti-rabbit conjugated to Alexa Fluor 488, 647, and 568 (Invitrogen). Secondary antibodies conjugated to PE (BD), Poly-L-Lysine (Sigma-Aldrich), cell tracker chloromethyl aminocoumarin (CMAC; Invitrogen), FluoSpheres biotin-labeled fluorescent (yellow-green fluorescent) microspheres 1 μm diameter (Invitrogen), fluorescently tagged streptadavin (Invitrogen). Ammonium chloride (NH_4Cl) and 1400W (Sigma-Aldrich), pepstatin A; manganese (III) tetrakis (4-benzoic acid) porphyrin (MnTBAP); N-acetylcysteine (NAC); and L -NG-Nitroarginine Methyl Ester (L-NAME) were gifts from Prof. J. Serrador, J.L. Rodriguez, and M. Ortiz de Landazuri.

Gentamicin Survival Assay

To determine the number of bacteria entering the cells, we followed the method described by Pizarro-Cerda and Cossart (2010), with some modifications. The indicated cells were infected with bacteria at moi of 10 for 1 hr at 37°C. After infections, 100 μg/ml of gentamicin was added, and samples were incubated for an additional 1 hr at 37°C (in the case of *E. coli* 200 μg/ml of gentamicin were used). Then, infected cells were washed with PBS to remove the antibiotic, counted, and lysed with 0.05% Triton X-100 (Sigma) in distilled water. Dilutions were seeded in LB (*Salmonella*) or BHI (*Staphylococcus* and *Listeria*) agar plates. CFUs were counted.

DC-T Cell Conjugate Formation

mDCs and hDCs were loaded with 10 μg/ml OVAp and 1 μg/ml SEE, respectively, and infected with bacteria for 1 hr. After extensive washing with PBS, infected DCs were coincubated with $CD4^+$ T cells from transgenic OTII mice or human enriched-$V\beta8^+$ T lymphoblasts.

Immunofluorescence Microscopy

DC-T cell conjugates were fixed with 4% paraformaldehyde in PBS. Samples were blocked with anti-mouse-CD16/CD32 monoclonal antibody (2.5 μg/ml) for 15 min in the case of mouse samples or human γ-globulin (100 μg/ml) in the case of human cells. After permeabilization (0.1% Triton X-100 in PBS), bacteria were detected by using specific antibodies or by its GFP expression. Depending on the experiment, DCs or T cells were marked with cell tracker chloromethyl aminocoumarin (CMAC). F-actin was detected using fluorescently tagged phalloidin. Samples were visualized by confocal microscopy using a Leica TCS-SP5 microscope equipped with 63× lens and controlled by Leica LAS AF. The images were analyzed with ImageJ (1.47; http://rsb.info.nih.gov/ij/).

Live-Cell Imaging

DCs were infected with GFP-expressing bacteria before conjugate formation. Infected DCs were resuspended in HBSS containing 2% FCS and seeded in glass-bottomed dish previously covered with poly-l-lysine. Then samples were coincubated with $CD4^+$ T cells from transgenic OTII mice or human enriched-$V\beta8^+$ T lymphoblasts, which were marked with CMAC. Conjugate formation was followed by fluorescence microscopy using a wide-field microscope (DMIRE2; Leica) with a 63× objective, illuminated with LEDs (CoolLed pE excitation system; CoolLed) and controlled by Leica MM AF (powered by Metamorph). Temperature (37°C) and CO_2 concentration (5%) were maintained stable during the image acquisition using Tempcontol 37-2 and CTI-controller 3700 (Leica).

Cryo-SXT

DC-T cell conjugates were seeded on gold quantifoil R 2/2 holey film microscopy grids (Au-HZB2 and Au-G200F1) coated with poly-L-lysine for 30 min. Samples were vitrified by plunge freezing. Vitrified grids were transfer to U41-TXM (HZB-BESSYII) (Schneider et al., 2012) and Mistral (ALBA-Light Source) (Pereiro et al., 2009) beamlines in BESSY II and ALBA synchrotron, respectively. The acquisition scheme was similar in both microscopes, using X-rays with 510 eV and 520 photon energy, respectively, and X-ray projections taken at liquid nitrogen temperature with 1° tilt steps. The zone plate objectives of both microscopes have an outermost zone width of 40 nm; alignment reconstruction and segmentation were performed as described in Chichón et al. (2012).

Bacteria Transinfection Assays

DC-T cell conjugate formation was performed in the presence (or absence) of polycarbonate filter-containing chambers of 3 μm pore size (Costar), with T cells in the bottom and infected DCs in the top of the chamber. As control, we also performed direct infections (moi = 10) of T cells. After 30 min of cell conjugates, gentamicin (100 μg/ml) was added for 1 hr, and then T cells were reisolated by a negative selection in auto-MACS Pro Separator. Cell purity was checked by flow cytometry. Infections of T cells and DC were assessed by classical gentamicin survival assays. CFUs corresponding to low DC contamination were subtracted. Only experiments with T cell purity >97% were taken into account. When indicated, $CD4^+$ T cells from OT-II mice were activated O/N with antigen-loaded APCs. Antibodies against LFA-1 or isotype controls were added for 15 min at 37°C before conjugate formation when indicated. In experiments involving listeria-OVA, DCs were not loaded with OVAp, and infection was performed for 6 hr (to allow antigen presentation) before conjugate formation. Gentamicin was added after 3 hr to avoid bacterial replication in the medium.

Transinfection was also tested by flow cytometry. Mouse T cells were stained with CMAC to be discriminated with respect to DC cells, which were labeled with CD11c-PE. hDCs cells were stained with anti-DC-SIGN in contrast to T cells responding to SEE, which were labeled with anti-vβ8. Extracellular bacteria were detected with anti-*S. enterica*, anti-*S. aureus*, or anti-*L. monocytogenes*) before fixation and permeabilization. Total bacteria (intracellular + extracellular) were detected by its GFP expression or by using antibodies after cellular permeabilization. Fluorochromes detecting extracellular bacteria were different than those marking total bacteria. Samples were then analyzed using a FACSCanto flow cytometer (BD Biosciences), and data were evaluated using FlowJo software (Tree Star, Ashland, OR). The same approach was followed using fluorescent, biotin-labeled microspheres.

Cellular Aggregation Using Anti-CD43 Antibody

DC-T cell conjugates were incubated with mAb against CD43, a control mAb IgG, or with PBS for 30 min at 37°C. Then dithiothreitol (DTT; 100 mM) was added for 10 min to allow cell disaggregation, followed by extensive vortexing. Finally, $CD4^+$ T cells were reisolated by negative selection, and CFUs were counted by gentamicin assay.

Analysis of Cytokine Production by Transinfected T Cells

OT-II T cells were mixed with infected or noninfected OVAp-loaded DCs (1:1 T cell/DC ratio) for 24 hr. After 24 hr conjugation, DCs were severely damaged by bacteria, contrary to T cells that resulted undamaged as revealed by propidium iodide and cell trace calcein violet (data not shown). Then $CD4^+$ T cells were reisolated by negative selection and activated with 5 μg/ml of anti-CD3 and 2 μg/ml of anti-CD28 for 72 hr. Phorbol myristate acetate (PMA; 50 ng/ml) was added for 6 hr, and supernatants were collected for cytokine quantification. Extracellular cytokines were quantified by CBA.

Adoptive Transfer Experiments

Transinfected OT-II $CD4^+$ T cells, noninfected OT-II $CD4^+$ T cells, noninfected WT $CD4^+$ T cells, or PBS (as a control) was injected i.v. into recipient WT mice. After 24 hr, mice were infected i.v. with *Listeria-OVA* (30 000 bacteria/mouse). Twenty-four or 48 hr after bacterial challenge, CFUs from spleen and liver were counted in agar plates.

Statistical Analysis

All statistical analyses were performed using GraphPad Prism software. When analyzing more than two groups, we used one-way analysis of variance (ANOVA), and multiple mean comparisons were corrected with Tukey post-test. Student's t test was used when individual comparisons of the mean between two groups were performed. Differences were considered significant at $p \leq 0.05$. Data are shown in column bars representing the mean ± SD of at least three independent experiments unless otherwise indicated.

SUPPLEMENTAL INFORMATION

Supplemental Information includes six figures and eight movies and can be found with this article at http://dx.doi.org/10.1016/j.chom.2014.04.006.

ACKNOWLEDGMENTS

We are grateful to Professor Pascale Cossart, Professor Iñigo Lasa, Dr. Pilar Martín, Dr. Jose Luis Rodriguez, Professor Manuel Ortiz de Landazuri, Dr. Juan Serrador, Dr. Dirk Brockstedt, and Bernhard Ryffel for providing us reagents. We also appreciated help from Dr. Miguel Vicente-Manzanares, Dr. María Yáñez-Mo, Dr. Laura Díaz-Muñoz, Marta Ramirez-Huesca, Adrian Izquierdo-Martínez, Raquel García-Ferreras, Dr. Stephan Werner, Dr. Katja Henzler, Dr. Andrea Sorrentino, and Dr. Stefan Rehbein. We thank HZB and ALBA for the allocation of synchrotron radiation beamtimes. The research leading to these results has received funding from Spanish BFU2011-29450, BFU2011-29038, FIS 11/00128, and SAF2011-25834, the European Community's Seventh Framework Programme (FP7/2007-2013) under BioStruct-X (grant agreement number 283570).

Received: April 18, 2013
Revised: January 18, 2014
Accepted: March 16, 2014
Published: May 14, 2014

REFERENCES

Balestrino, D., Hamon, M.A., Dortet, L., Nahori, M.A., Pizarro-Cerda, J., Alignani, D., Dussurget, O., Cossart, P., and Toledo-Arana, A. (2010). Single-cell techniques using chromosomally tagged fluorescent bacteria to study Listeria monocytogenes infection processes. Appl. Environ. Microbiol. *76*, 3625–3636.

Barnden, M.J., Allison, J., Heath, W.R., and Carbone, F.R. (1998). Defective TCR expression in transgenic mice constructed using cDNA-based alpha- and beta-chain genes under the control of heterologous regulatory elements. Immunol. Cell Biol. *76*, 34–40.

Bregenholt, S., Berche, P., Brombacher, F., and Di Santo, J.P. (2001). Conventional alpha beta T cells are sufficient for innate and adaptive immunity against enteric Listeria monocytogenes. J. Immunol. *166*, 1871–1876.

Calabia-Linares, C., Robles-Valero, J., de la Fuente, H., Perez-Martinez, M., Martín-Cofreces, N., Alfonso-Pérez, M., Gutierrez-Vázquez, C., Mittelbrunn, M., Ibiza, S., Urbano-Olmos, F.R., et al. (2011). Endosomal clathrin drives actin accumulation at the immunological synapse. J. Cell Sci. *124*, 820–830.

Campanero, M.R., del Pozo, M.A., Arroyo, A.G., Sánchez-Mateos, P., Hernández-Caselles, T., Craig, A., Pulido, R., and Sánchez-Madrid, F. (1993). ICAM-3 interacts with LFA-1 and regulates the LFA-1/ICAM-1 cell adhesion pathway. J. Cell Biol. *123*, 1007–1016.

Cemerski, S., and Shaw, A. (2006). Immune synapses in T-cell activation. Curr. Opin. Immunol. *18*, 298–304.

Charpentier, E., Anton, A.I., Barry, P., Alfonso, B., Fang, Y., and Novick, R.P. (2004). Novel cassette-based shuttle vector system for gram-positive bacteria. Appl. Environ. Microbiol. *70*, 6076–6085.

Chichón, F.J., Rodríguez, M.J., Pereiro, E., Chiappi, M., Perdiguero, B., Guttmann, P., Werner, S., Rehbein, S., Schneider, G., Esteban, M., and Carrascosa, J.L. (2012). Cryo X-ray nano-tomography of vaccinia virus infected cells. J. Struct. Biol. *177*, 202–211.

Cormack, B.P., Valdivia, R.H., and Falkow, S. (1996). FACS-optimized mutants of the green fluorescent protein (GFP). Gene *173* (1 Spec No), 33–38.

Cossart, P. (2011). Illuminating the landscape of host-pathogen interactions with the bacterium Listeria monocytogenes. Proc. Natl. Acad. Sci. USA *108*, 19484–19491.

Cossart, P., and Sansonetti, P.J. (2004). Bacterial invasion: the paradigms of enteroinvasive pathogens. Science *304*, 242–248.

Dai, W.J., Köhler, G., and Brombacher, F. (1997). Both innate and acquired immunity to Listeria monocytogenes infection are increased in IL-10-deficient mice. J. Immunol. *158*, 2259–2267.

Dustin, M.L. (2008). T-cell activation through immunological synapses and kinapses. Immunol. Rev. *221*, 77–89.

Ehlers, S., Mielke, M.E., Blankenstein, T., and Hahn, H. (1992). Kinetic analysis of cytokine gene expression in the livers of naive and immune mice infected with Listeria monocytogenes. The immediate early phase in innate resistance and acquired immunity. J. Immunol. *149*, 3016–3022.

Geijtenbeek, T.B., Kwon, D.S., Torensma, R., van Vliet, S.J., van Duijnhoven, G.C., Middel, J., Cornelissen, I.L., Nottet, H.S., KewalRamani, V.N., Littman, D.R., et al. (2000). DC-SIGN, a dendritic cell-specific HIV-1-binding protein that enhances trans-infection of T cells. Cell *100*, 587–597.

Gomez, T.S., Hamann, M.J., McCarney, S., Savoy, D.N., Lubking, C.M., Heldebrant, M.P., Labno, C.M., McKean, D.J., McNiven, M.A., Burkhardt, J.K., and Billadeau, D.D. (2005). Dynamin 2 regulates T cell activation by controlling actin polymerization at the immunological synapse. Nat. Immunol. *6*, 261–270.

Hogquist, K.A., Jameson, S.C., Heath, W.R., Howard, J.L., Bevan, M.J., and Carbone, F.R. (1994). T cell receptor antagonist peptides induce positive selection. Cell *76*, 17–27.

Inaba, K., Inaba, M., Romani, N., Aya, H., Deguchi, M., Ikehara, S., Muramatsu, S., and Steinman, R.M. (1992). Generation of large numbers of dendritic cells from mouse bone marrow cultures supplemented with granulocyte/macrophage colony-stimulating factor. J. Exp. Med. *176*, 1693–1702.

Izquierdo-Useros, N., Naranjo-Gómez, M., Erkizia, I., Puertas, M.C., Borràs, F.E., Blanco, J., and Martinez-Picado, J. (2010). HIV and mature dendritic cells: Trojan exosomes riding the Trojan horse? PLoS Pathog. *6*, e1000740.

Kaufmann, S.H., and Schaible, U.E. (2005). Antigen presentation and recognition in bacterial infections. Curr. Opin. Immunol. *17*, 79–87.

McElroy, D.S., Ashley, T.J., and D'Orazio, S.E. (2009). Lymphocytes serve as a reservoir for Listeria monocytogenes growth during infection of mice. Microb. Pathog. *46*, 214–221.

Mittelbrunn, M., and Sánchez-Madrid, F. (2012). Intercellular communication: diverse structures for exchange of genetic information. Nat. Rev. Mol. Cell Biol. *13*, 328–335.

Müller, A.J., Filipe-Santos, O., Eberl, G., Aebischer, T., Späth, G.F., and Bousso, P. (2012). CD4+ T cells rely on a cytokine gradient to control intracellular pathogens beyond sites of antigen presentation. Immunity *37*, 147–157.

Nakane, A., Numata, A., and Minagawa, T. (1992). Endogenous tumor necrosis factor, interleukin-6, and gamma interferon levels during Listeria monocytogenes infection in mice. Infect. Immun. *60*, 523–528.

Niedergang, F., Dautry-Varsat, A., and Alcover, A. (1998). Cooperative activation of TCRs by enterotoxin superantigens. J. Immunol. *161*, 6054–6058.

Oykhman, P., and Mody, C.H. (2010). Direct microbicidal activity of cytotoxic T-lymphocytes. J. Biomed. Biotechnol. *2010*, 249482.

Pereiro, E., Nicolás, J., Ferrer, S., and Howells, M.R. (2009). A soft X-ray beamline for transmission X-ray microscopy at ALBA. J. Synchrotron Radiat. *16*, 505–512.

Pizarro-Cerda, J., and Cossart, P. (2010). Listeria monocytogenes: techniques to analyze bacterial infection in vitro. In Cell Biology Assays: Essential Methods, G. Kreitzer, J. Fanny, and C. Espenel, eds. (New York: Elsevier), pp. 261–272.

Pope, C., Kim, S.K., Marzo, A., Masopust, D., Williams, K., Jiang, J., Shen, H., and Lefrançois, L. (2001). Organ-specific regulation of the CD8 T cell response to Listeria monocytogenes infection. J. Immunol. *166*, 3402–3409.

Reichardt, P., Dornbach, B., and Gunzer, M. (2010). APC, T cells, and the immune synapse. Curr. Top. Microbiol. Immunol. *340*, 229–249.

Saito, T., and Batista, F.D. (2010). Immunological Synapse. (New York: Springer).

Salgado-Pabón, W., Celli, S., Arena, E.T., Nothelfer, K., Roux, P., Sellge, G., Frigimelica, E., Bousso, P., Sansonetti, P.J., and Phalipon, A. (2013). Shigella impairs T lymphocyte dynamics in vivo. Proc. Natl. Acad. Sci. USA *110*, 4458–4463.

Sallusto, F., and Lanzavecchia, A. (1994). Efficient presentation of soluble antigen by cultured human dendritic cells is maintained by granulocyte/macrophage colony-stimulating factor plus interleukin 4 and downregulated by tumor necrosis factor alpha. J. Exp. Med. *179*, 1109–1118.

Sanchez-Madrid, F., Simon, P., Thompson, S., and Springer, T.A. (1983). Mapping of antigenic and functional epitopes on the alpha- and beta-subunits of two related mouse glycoproteins involved in cell interactions, LFA-1 and Mac-1. J. Exp. Med. *158*, 586–602.

Sánchez-Mateos, P., Campanero, M.R., del Pozo, M.A., and Sánchez-Madrid, F. (1995). Regulatory role of CD43 leukosialin on integrin-mediated T-cell adhesion to endothelial and extracellular matrix ligands and its polar redistribution to a cellular uropod. Blood *86*, 2228–2239.

Schneider, G., Guttmann, P., Heim, S., Rehbein, S., Mueller, F., Nagashima, K., Heymann, J.B., Müller, W.G., and McNally, J.G. (2010). Three-dimensional cellular ultrastructure resolved by X-ray microscopy. Nat. Methods *7*, 985–987.

Schneider, G., Guttmann, P., Rehbein, S., Werner, S., and Follath, R. (2012). Cryo X-ray microscope with flat sample geometry for correlative fluorescence and nanoscale tomographic imaging. J. Struct. Biol. *177*, 212–223.

Serrador, J.M., Nieto, M., Alonso-Lebrero, J.L., del Pozo, M.A., Calvo, J., Furthmayr, H., Schwartz-Albiez, R., Lozano, F., González-Amaro, R., Sánchez-Mateos, P., and Sánchez-Madrid, F. (1998). CD43 interacts with moesin and ezrin and regulates its redistribution to the uropods of T lymphocytes at the cell-cell contacts. Blood *91*, 4632–4644.

Solano, C., García, B., Valle, J., Berasain, C., Ghigo, J.-M., Gamazo, C., and Lasa, I. (2002). Genetic analysis of Salmonella enteritidis biofilm formation: critical role of cellulose. Mol. Microbiol. *43*, 793–808.

Steinman, R.M. (1991). The dendritic cell system and its role in immunogenicity. Annu. Rev. Immunol. *9*, 271–296.

Ueda, H., Morphew, M.K., McIntosh, J.R., and Davis, M.M. (2011). CD4+ T-cell synapses involve multiple distinct stages. Proc. Natl. Acad. Sci. USA *108*, 17099–17104.

Vaudaux, P., and Waldvogel, F.A. (1979). Gentamicin antibacterial activity in the presence of human polymorphonuclear leukocytes. Antimicrob. Agents Chemother. *16*, 743–749.

Vergara-Irigaray, M., Valle, J., Merino, N., Latasa, C., García, B., Ruiz de Los Mozos, I., Solano, C., Toledo-Arana, A., Penadés, J.R., and Lasa, I. (2009). Relevant role of fibronectin-binding proteins in Staphylococcus aureus biofilm-associated foreign-body infections. Infect. Immun. *77*, 3978–3991.

Waite, J.C., Leiner, I., Lauer, P., Rae, C.S., Barbet, G., Zheng, H., Portnoy, D.A., Pamer, E.G., and Dustin, M.L. (2011). Dynamic imaging of the effector immune response to listeria infection in vivo. PLoS Pathog. *7*, e1001326.